Received: 3 November 2020 | Accepted: 2 February 2021 | Published on: 4 March 2021

DOI: 10.1002/asna.202123856

Astronomische Nachrichten

ORIGINAL ARTICLE

Radius, rotational period, and inclination of the Be stars in the Be/gamma-ray binaries MWC 148 and MWC 656

Radoslav K. Zamanov[1] | Kiril A. Stoyanov[1] | Josep Mart[2] | Vladislav D. Marchev[1] | Yanko M. Nikolov[1]

[1]Institute of Astronomy and National Astronomical Observatory, Bulgarian Academy of Sciences, Sofia, Bulgaria

[2]Departamento de Física, Escuela Politécnica Superior de Jaén, Universidad de Jaén, Jaén, Spain

Correspondence
Radoslav K. Zamanov, Institute of Astronomy and National Astronomical Observatory, Bulgarian Academy of Sciences, Tsarigradsko Shose 72, BG-1784 Sofia, Bulgaria.
Email: rkz@astro.bas.bg

Funding information
Programme "Young scientists and postdoctoral students", Bulgarian Ministry of Education and Science, Grant/Award Number: DCM 577/17.08.2018; Consejera de Economa, Innovación, Ciencia y Empleo of Junta de Andaluca as research group, Grant/Award Number: FQM- 322; Spanish Ministerio de Ciencia, Innovación y Universidades, Grant/Award Number: PID2019-105510GB-C32 / AEI / 10.13039/501100011033; Bulgarian National Science Fund, Grant/Award Number: КП-06-H28/2; Binary stars with compact object

Abstract

Using TESS photometry and Rozhen spectra of the Be/γ-ray binaries MWC 148 and MWC 656, we estimate the projected rotational velocity ($v \sin i$), rotational period ($P_{\rm rot}$), radius (R_1), and inclination (i) of the mass donor. For MWC 148, we derive $P_{\rm rot} = 1.10 \pm 0.03$ day, $R_1 = 9.2 \pm 0.05$ $R_{\rm sun}$, $i = 40° \pm 2°$, and $v \sin i = 272 \pm 5$ km s^{-1}. For MWC 656, we obtain $P_{\rm rot} = 1.12 \pm 0.03$ day, $R_1 = 8.8 \pm 0.5$ $R_{\rm sun}$, $i = 52° \pm 3°$, and $v \sin i = 313 \pm 3$ km s^{-1}. For MWC 656, we also find that the rotation of the mass donor is coplanar with the orbital plane.

KEYWORDS

stars: emission line, Be, binaries: spectroscopic, gamma rays: stars, stars: individual: MWC 148, MWC 656

1 | INTRODUCTION

The γ-ray binaries are a recently established and rare subclass of the high-mass X-ray binaries with most of their luminosity output being radiated above 1 MeV (Chernyakova & Malyshev 2020; Dubus 2013). They are composed of an OBe donor star and a neutron star or a black hole (Mirabel 2012). The mechanism responsible for the high-energy emission in these systems is still a subject of debate. The γ-rays could be produced

Data from TESS and Rozhen

either by accretion-driven jets or by the rotation-powered strong pulsar winds interacting with the nearby medium (Dubus 2006; Massi & Jaron 2013; Romero et al. 2007), and/or by a neutron star in the propeller regime (Wang & Robertson 1985).

So far, seven systems have been confirmed as γ-ray binaries: PSR B1259-63 (Aharonian et al. 2005a), LS 5039 (Aharonian et al. 2005b), LS I + 61,303 (Albert et al. 2006), HESS J0632 + 057 (Aharonian et al. 2007), 1FGL J1018.6–5856 (Corbet et al. 2011), PSR J2032 + 4127 (Lyne et al. 2015) and LMC-P3 (Corbet et al. 2016). The nature of the compact object is already known in PSR B1259-63 and PSR J2032 + 4127, where radio observations have confirmed that they contain neutron stars (Abdo et al. 2009; Johnston et al. 1992). Based on the donor star and the presence of a circumstellar disk, two subgroups of γ-ray binaries have been proposed. The first subgroup harbors an O-type donor star and shows a single-peak profile in their γ-ray light curve. The second subgroup contains an OBe star and shows several peaks in their light curves, occasionally correlated with the times when the compact object crosses and in some cases truncates the circumstellar disk of the donor star (Paredes & Bordas 2019).

MWC 148 (HD 259440) was identified as the optical counterpart of the variable TeV source HESS J0632 + 057 (Aharonian et al. 2007) and also detected in the GeV domain (Li et al. 2017). The system consists of a B0Vpe star (Casares et al. 2012) and a compact object, with an orbital period $P_{\rm orb} = 315^{+6}_{-4}$ days (Aliu et al. 2014).

MWC 656 (HD 215227) is the suspected optical counterpart of the γ-ray source AGL J2241 + 4454 detected by the *AGILE* satellite above 100 MeV (Lucarelli et al. 2010; Williams et al. 2010). It is the first discovered binary containing a black hole as a companion of a Be star (Casares et al. 2014). MWC 656 was only occasionally detected at GeV energies (Aleksić et al. 2015). The black hole nature of the compact object renders it similar to the typical γ-ray binaries. The orbital period of the system, obtained by optical photometry and later confirmed by radial velocity measurements, is $P_{\rm orb} = 60.37 \pm 0.04$ d (Casares et al. 2014; Williams et al. 2010).

Here, using photometric and spectral observations, we estimate the rotational period, radius, and inclination of the mass donors in the Be/γ-ray binaries MWC 148 and MWC 656.

2 | OBSERVATIONS

We use both space photometry and ground-based spectra.

2.1 | TESS photometric data

The *Transiting Exoplanet Survey Satellite* (*TESS*, Ricker et al. 2015) is a space-based optical telescope launched in 2018 with the primary mission to perform an all-sky survey to search for transiting exoplanets. In order to fulfill the mission, the sky is divided into a number of *sectors*, each of which corresponds to the total field of view of all four cameras of the telescope, namely $24° \times 96°$. Each sector is observed for approximately 27 days at a cadence of 2 min. Simple aperture photometry is applied to each of the data files to obtain a barycentered light curve file of the selected object. The bandpass of *TESS* is centered on the classical I_c filter, but it is wider and spans from 6,000 to 10,000 Å: in other words, the telescope observes the red and the near-infrared emissions of the stars. The light curves of MWC 656 and MWC 148 were downloaded from the Mikulski Archive for Space Telescopes archives.[1]

2.2 | Rozhen spectral data

The spectral observations were obtained with the ESPERO spectrograph of the 2.0-m RCC telescope at Rozhen National Astronomical Observatory located in Rhodope Mountain, Bulgaria. ESPERO is a fiber-fed Echelle spectrograph giving a dispersion of 0.06 Å px^{-1} and resolving power ∼30, 000 at 6,560 Å (Bonev et al. 2017). The spectral processing and measurements of the spectral lines are performed using standard routines provided by IRAF (Tody 1993). On each spectrum we measure the equivalent width EW (Hα) and the full width at half-maximum (FWHM) of the Hα emission line, equivalent width EW(5316) and the full width at zero intensity (FWZI) of the FeII 5316 Å line. FWZI is the full width of the emission line at the continuum level. Examples of the emission lines are presented in Figure 1. They are normalized to the local continuum. The typical errors of our measurements are ±5% in EW(Hα), ±7 km s^{-1} in FWHM(Hα), ±10% in EW(FeII5316), and ±40 km s^{-1} in FWZI(FeII). The log of observations is given in Table 1.

Traces of residual wings due to photospheric absorption were not detected, and the interpolated continuum was taken as the baseline during the measurements of EW and FWHM. The equivalent width is measured using *splot* routine in IRAF by marking two continuum points around the line to be measured. The linear continuum is subtracted and the flux determined by simply summing the pixels with partial pixels at the ends. The method

[1] https://archive.stsci.edu/tess/

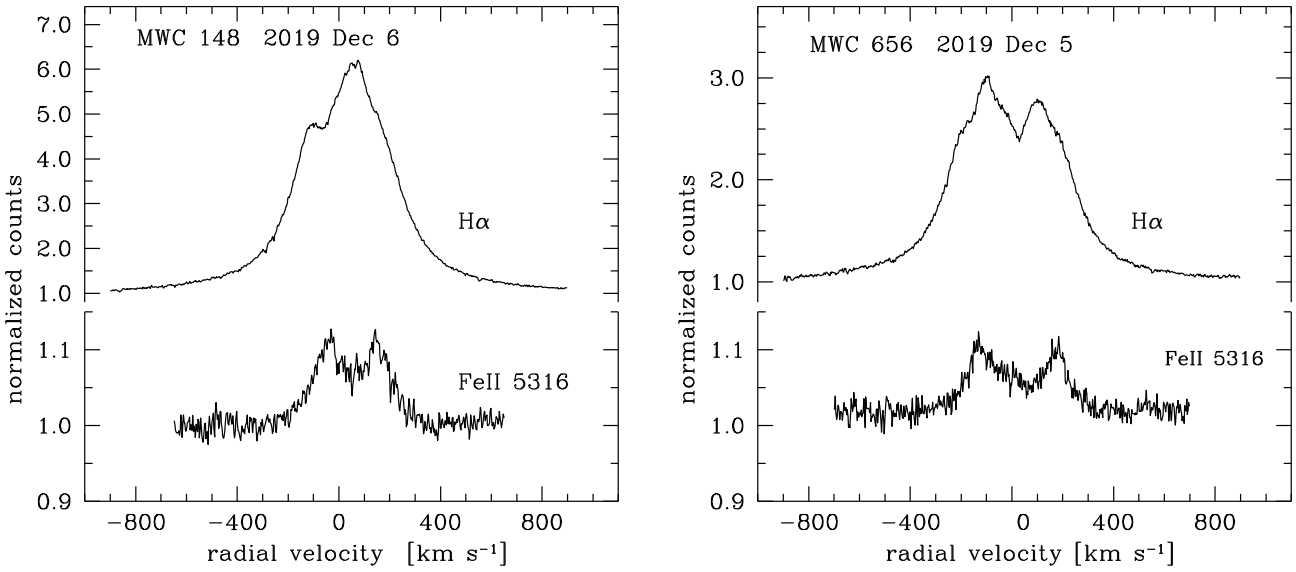

FIGURE 1 Emission lines *Hα* and FeII 5316 in the spectra of MWC 148 (left panel) and MWC 656 (right panel)

TABLE 1 Spectroscopic observations of MWC 148 and MWC 656

Object	Date-obs. yyyy-mm-dd:hh:mm	Exp.-time (s)	S/N	EW(Hα) (Å)	FWHM(Hα) (km s^{-1})	EW(FeII5316) (Å)	FWZI(FeII) (km s^{-1})
MWC 148	2019-02-20T18:45	2,400	75	−46.9	411	−0.59	672
MWC 148	2019-12-06T01:45	2,400	95	−46.4	405	−0.60	711
MWC 148	2020-01-16T21:16	3,600	70	−44.8	418	−0.59	683
MWC 148	2020-09-06T02:01	1,800	60	−43.7	412	−0.57	709
MWC 656	2019-08-22T20:10	3,600	90	−20.9	493	−0.48	705
MWC 656	2019-12-05T17:48	2,400	100	−21.6	491	−0.54	722
MWC 656	2020-09-05T21:50	3,600	64	−21.7	490	−0.60	700

Note: In the table are given the date of observations, UT start, exposure time in seconds, signal-to-noise ratio at about 6600 Å, EW(Hα), FWHM(*Hα*), EW(FeII5316), and FWZI(FeII5316).

calculates the area under the profile irrespective of its shape (e.g., Mathew & Subramaniam 2011). The FWHM is measured by identifying the points of the emission line profile where the intensity is equal to one-half of the peak intensity, as shown in Glebocki et al. (1986, Fig. 1). The horizontal distance between this two points was measured. This measurement also does not depend on the profile shape.

3 | ANALYSIS METHODOLOGY

In this section we give the equations connecting the relevant parameters of the primary components on which our estimates are based. For the Be stars, Hanuschik (1989) gives a relation between projected rotational velocity (v sin i), FWHM(Hα), and EW(Hα). We use his relation in the form

$$v \sin i = 0.813\,(\mathrm{FWHM}\,10^{0.08\log \mathrm{EW(H\alpha)}-0.14} - 70), \quad (1)$$

where FWHM and v sin i are measured in km s^{-1} and EW(Hα) is in Å.

The FeII lines are optically thin and their profiles reflect the Keplerian rotation in the innermost part of the Be disk (Hanuschik 1996). The inclination of the Be star is connected with the full width at zero intensity of the FeII lines and its radius:

$$\frac{\mathrm{FWZI}}{2\sin i} = \left(\frac{GM_1}{(1+\varepsilon)R_1}\right)^{1/2}, \quad (2)$$

where G is the gravitational constant, M_1 is the mass of the Be star, R_1 is its radius, i is the inclination of the Be star

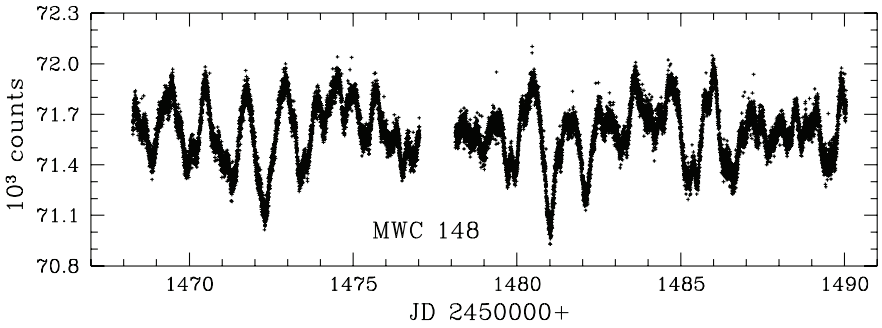

FIGURE 2 TESS light curve of MWC 148

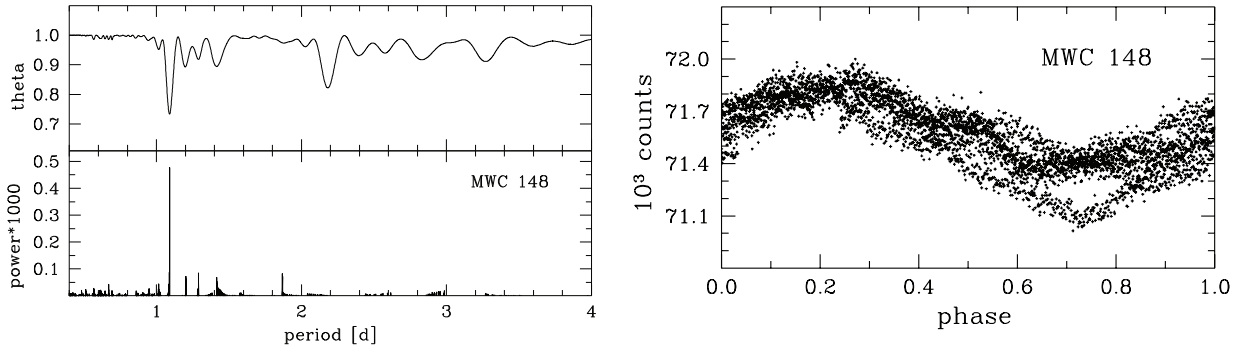

FIGURE 3 *Left panel*: periodogram analysis for MWC 148—theta and power versus period. *Right panel*: the light curve during 1,468–1,474 folded with a 1.156 day period

to the line of sight, ε is a dimensionless parameter ($\varepsilon \geq 0$). Equation (2) represents the Keplerian motion in the disk and is a modification of that used in Casares et al. (2012, Sect.6.1). The region where the FeII lines are produced can be extended down to the very surface of the Be star or close to it. The parameter ε, for which we adopt $0 \leq \varepsilon < 0.1$, represents how close to the surface of star the emission at FWZI of the FeII lines is formed.

The rotational period of the Be star is also connected with the above parameters:

$$P_{\rm rot} = \frac{2\pi R_1}{v \sin i} \sin i. \quad (3)$$

The rotational periodicity is probably due to the interaction between the magnetic field of the Be star and its circumstellar disk or to the presence of some physical feature, such as a spot or cloud, co-rotating with the star (Smith et al. 2006). The rotational periods in the Be/γ-ray binaries are expected to be of the order of 1 day (Zamanov et al. 2016b1.16).

The applied methodology involves the following steps:

1. A periodogram analysis of the TESS data is performed to estimate $P_{\rm rot}$.
2. The parameter $v \sin i$ is estimated using Equation (1) and the data in Table 1.
3. A mass value for the Be star is adopted according to its spectral type.
4. Using Equations (2) and (3), the values of R_1 and i are calculated for the primaries of MWC 148 and MWC 656.

The period-search methods applied to the TESS photometry were the phase dispersion minimization, PDM (Stellingwerf 1978) and the CLEAN algorithm (Roberts et al. 1987).

4 | MWC 148

TESS photometry for MWC 148, in the interval JD 2451468.2–JD 2451490.0, can be accessed under Input Catalogue ID 234929785 and is plotted in Figure 2. The periodogram analysis is presented in the left panel of Figure 3, where the PDM statistic (theta) and the CLEAN component amplitude are plotted. Over the entire data set, the analysis yields $P_{\rm rot} = 1.0908 \pm 0.0002$ day. The periodyogram analysis of the data in the (JD − 2450000) time interval 1,468–1,490 gives a clear period of 1.09 ± 0.03 day, in the interval 1,468–1,477 a clear period of 1.131 ± 0.025 day, and in the interval 1,478–1,490 a clear period of 1.075 ± 0.025 day. A visual inspection of the data gives us the possibility to select the parts of the light curve where this periodicity is most clearly visible. Using days 1468–1474, we find 1.156 day, and for days 1479–1487 we find 1.101 day. The light curve for days 1,468–1,474 is plotted in the right panel of Figure 3. We consider that the

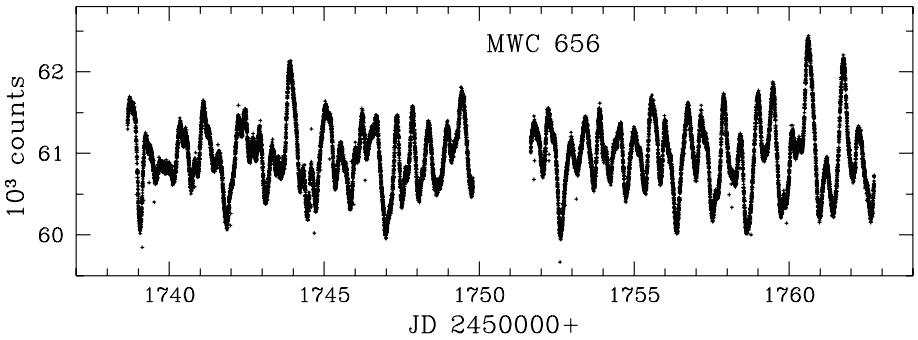

FIGURE 4 TESS light curve of MWC 656

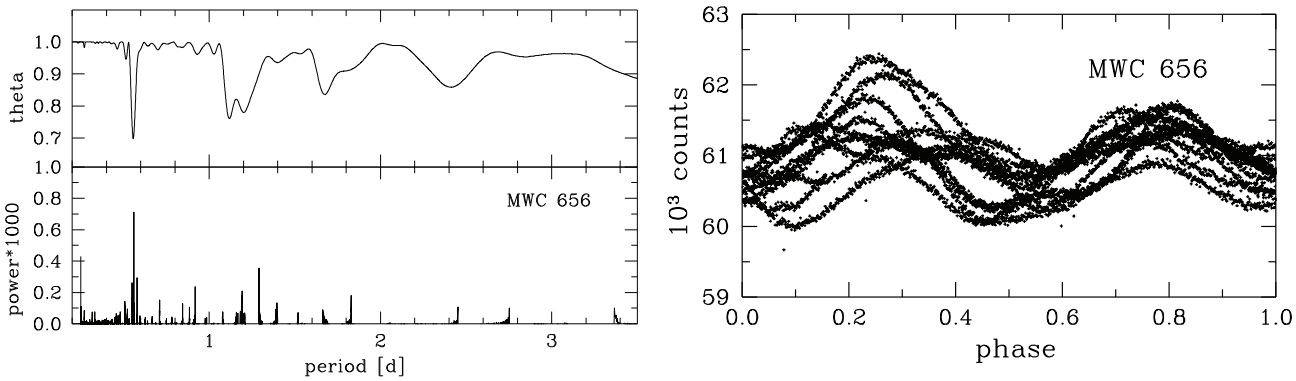

FIGURE 5 *Left panel*: periodogram analysis for MWC 148. The most significant period is 0.559 day. *Right panel*: the light curve during 1,751–1,763 folded with a 1.117 day period, which is probably the rotational period of the B star

rotational period of the Be star in MWC 148 is in the range $1.09 \leq P_{rot} < 1.16$ day.

Using Equation (1) and the values given in Table 1, we find $v \sin i = 272 \pm 5$ km s^{-1}. Casares et al. (2012) give a spectral type B0Vpe. A B0V star is expected to have on average mass $M_1 = 15.0 \pm 0.5\ M_{sun}$ (Hohle et al. 2010). For MWC 148, Aragona et al. (2010) derived $M_1 = 13.2$–$19.0\ M_e$ from spectral model fits, which is in agreement with the adopted $M_1 = 15.0\ M_{sun}$. Adopting FWZI(λ5316) ≈694 km s^{-1} and v sin $i = 272$ km s^{-1}, we find $i = 40° \pm 2°$ and $R_1 = 9.2 \pm 0.5\ R_{sun}$.

It is worth noting for comparison that (i) a B0V star is expected to have $R_1 = 7.2\ R_\odot$ (Straizys & Kuriliene 1981); (ii) Casares et al. (2012) give FWZI(λ5018) ∼1300 km s^{-1} and $v \sin i = 373$ km s^{-1}; (iii) $v \sin i = 430$ km s^{-1} (Gutiérrez-Soto et al. 2007) and $v \sin i = 500$ km s^{-1} (Aragona et al. 2010) are reported for this object.

5 | MWC 656

TESS photometry for MWC 656 (HD 215227), in the interval JD 2451738–2451763 can be accessed under Input Catalogue ID 153880067 (Figure 4). The data gap is due to the telescope being repointed to transfer data to Earth at this time. The periodogram analysis is shown in the left panel of Figure 5 with the same kind of plots as for the previous source. Over the entire data set, the analysis yields $P_{rot} = 0.5586 \pm 0.0002$ days. In contrast, we do not find a clear period in the (JD − 2450000) interval 1,738–1,751 days. However, in the interval 1,751.6–1,762.7 days, a clear period of 0.557 ± 0.025 days is detected. Looking at the interval 1,760–1,763 days, we see that there is a repetition of strong and weak maxima, which probably means that the rotational period is doubled to $P_{rot} = 1.117$ day.

For the primary, Williams et al. (2010) estimated $T_{eff} = 19{,}000 \pm 3{,}000$ K, log $g = 3.7 \pm 0.2$, $M_1 = 7.7 \pm 2.0\ M_{sun}$, and $R_1 = 6.6 \pm 1.9\ R_e$. Casares et al. (2014) found that the mass donor is a giant (B1.5–2 III) and gave a mass range 10–16 M_e. From the results of Hohle et al. (2010), such a star is expected to have $8.0 < M_1 < 10.0\ M_{sun}$.

Using the relation between $v \sin i$, FWHM($H\alpha$), and EW(Hα) (Equation (1)), and our values (see Table 1), we find $v \sin i = 313 \pm 3$ km s^{-1}, which is similar to the values 330 ± 30 km s^{-1} (Casares et al. 2014), 262 ± 26 km s^{-1} (Yudin 2001), and 330 ± 50 km s^{-1} (Williams et al. 2010).

We measured FWZI(FeII 5316) = 12.5–12.9 Å $= 709 \pm 12$ km s^{-1}, which is below the value FWZI(FeII 5018)∼1000 km s^{-1} (Casares et al. 2012).

Adopting $M_1 = 10.0 \pm 0.5\ M_{sun}$, $v \sin i = 313$ km s^{-1}, and $FWZI(\text{FeII}) = 709$ km s^{-1}, the system of Equations (2)

and (3) can be solved. As a result, we find $R_1 = 8.8 \pm 0.5$ $R_{\rm sun}$ and $i = 52° \pm 2°$. The obtained value of R_1 agrees with the estimates of the average radius for a B1.5–2 III star ($8.3 - 8.8$ $R_{\rm sun}$; Straizys & Kuriliene 1981).

For MWC 656, from the radial velocity measurements, Casares et al. (2014) obtained $M_1 \sin^3 i_{\rm orb} = 5.83 \pm 0.70$. For $M_1 = 10\,M_{\rm sun}$, this gives $53° < i_{\rm orb} < 60°$. It appears that the orbital plane and the equatorial plane of the Be star are practically coplanar within ±4°.

6 | DISCUSSION

In Be/X-ray binaries, the primary is a rapidly rotating Be star with mass ∼10 $M_{\rm sun}$ and the secondary is a neutron star or a black hole. The secondary mass is expected to be ∼2 $M_{\rm sun}$ for a neutron star, and ∼5 $M_{\rm sun}$ in the case of black hole. The orbital periods are in the range 10–400 days (Reig 2011). The Be/γ-ray binaries are a subgroup of the Be/X-ray binaries and should have similar binary parameters. They are a product of the evolution of a binary containing two moderately massive stars, which undergoes mass transfer from the originally more massive star towards its companion (Negueruela 2007; Pols et al. 1991). The eccentricities in these systems are caused by a kick to the compact object during the supernova explosion that formed it (e.g., Martin et al. 2009).

HESS J0632 + 057 (MWC 148) produces nonthermal radio, X-ray, GeV, and very high energy gamma-ray emission. The nonthermal emission is modulated with the 315 days orbital period and has a a peculiar light curve containing two peaks, separated by a dip—a sharp peak with a short decay before the apastron passage and a broad (several tens of days) secondary peak after the apastron passage in X-rays and TeV (Aliu et al. 2014; Archer et al. 2020). The nonthermal activity before and around apastron can be linked to (i) the accumulation of nonthermal particles in the vicinity of the binary, and the sudden drop of the emission before apastron is produced by the disruption of the two-wind interaction structure, allowing these particles to escape efficiently (Bosch-Ramon et al. 2017) or (ii) an accumulation of hot shocked plasma in the inner spiral arm, later released when the spiral arm is disrupted in the periastron–apastron direction (Barkov & Bosch-Ramon 2018).

For MWC 148, two solutions for the orbit indicate that it is highly eccentric: $e = 0.83 \pm 0.08$ (Casares et al. 2012) and $e = 0.64 \pm 0.29$ (Moritani et al. 2018). In our previous paper (Zamanov et al. 2017), we assumed the value of i, on the basis of the strong resemblance of the optical emission lines between MWC 148 and the bright Be star γ Cas (Zamanov et al. 2016a), for which the inclination is $i = 43° \pm 3°$ (Clarke 1990; Poeckert & Marlborough 1978). Our result here for MWC 148 ($i = 40° \pm 2°$) confirms the assumption that one of the reasons for this similarity is the inclination.

MWC 656 is faint in X-rays and it reaches the faintest X-ray luminosities ever detected in stellar-mass black holes (Ribó et al. 2017). It may not continuously emit γ-rays (Alexander & McSwain 2016). For this binary, Casares et al. (2014) found that the mass of the black hole is in the range 3.8–6.9 $M_\odot$. The orbital eccentricity is $e = 0.10 \pm 0.04$. It is suggested that the warp and precession observed in Be star disks may be caused by a misalignment between the spin axis of the Be star and the orbit of the binary companion (Martin et al. 2011). Our results indicate that there is no misalignment in MWC 656, and consequently warping and precession should not be observed.

The velocity kick from the supernova has two effects: it renders the orbit eccentric, and it misaligns the orbit with respect to the spin axis of the Be star. In systems that experience low velocity kicks, the misalignments tend to be small (Martin et al. 2011). The low orbital eccentricity and the alignment between the spin axis of the primary and the axis of the binary orbit indicate that the compact object in MWC 656 was born with low kick velocity.

7 | CONCLUSIONS

We evaluated some parameters for the mass donor stars in the Be/γ-ray binaries MWC 148 and MWC 656. For MWC 148, we estimate $v \sin i = 272 \pm 5$ km s^{-1}, $P_{\rm rot} = 1.10 \pm 0.03$ days, $R_1 = 9.2 \pm 0.05$ $R_{\rm sun}$, and $i = 40° \pm 2°$. For MWC 656, we obtain $v \sin i = 313 \pm 3$ km s^{-1}, $P_{\rm rot} = 1.12 \pm 0.03$ days, $R_1 = 8.8 \pm 0.5$ $R_{\rm sun}$, and $i = 52° \pm 3°$. These parameters should be useful for future accurate modeling of these systems.

ACKNOWLEDGMENTS

We are grateful to Mike Bode (Liverpool John Moores University) for a critical reading of the manuscript and an anonymous referee for useful comments. This work was supported by Bulgarian National Science Fund—project КП-06-H28/2 "Binary stars with compact object". JM acknowledges support by grant PID2019-105510GB-C32 / AEI / 10.13039/501100011033 from the Agencia Estatal de Investigación of the Spanish Ministerio de Ciencia, Innovación y Universidades, and by Consejera de Economa, Innovación, Ciencia y Empleo of Junta de Andaluca as research group FQM- 322, as well as FEDER funds. YMN acknowledges grant DCM 577/17.08.2018 from National Research Programme "Young scientists and postdoctoral students" of the Bulgarian Ministry of Education and Science.

REFERENCES

Abdo, A. A., Ackermann, M., Ajello, M., et al. 2009, *Science*, *325*, 840.

Aharonian, F., Akhperjanian, A. G., Aye, K.-M., et al. 2005a, *A&A*, *442*, 1.

Aharonian, F., Akhperjanian, A. G., Aye, K.-M., et al. 2005b, *Science*, *309*, 746.

Aharonian, F. A., Akhperjanian, A. G., Bazer-Bachi, A. R., et al. 2007, *A&A*, *469*, L1.

Albert, J., Aliu, E., Anderhub, H., et al. 2006, *Science*, *312*, 1771.

Aleksić, J., Ansoldi, S., Antonelli, L. A., et al. 2015, *A&A*, *576*, A36.

Alexander, M. J., & McSwain, M. V. 2016, *ASP Conf. Ser.*, *506*, 243.

Aliu, E., Archambault, S., Aune, T., et al. 2014, *ApJ*, *780*, 168.

Aragona, C., McSwain, M. V., & De Becker, M. 2010, *ApJ*, *724*, 306.

Archer, A., Benbow, W., Bird, R., et al. 2020, *ApJ*, *888*, 115.

Barkov, M. V., & Bosch-Ramon, V. 2018, *MNRAS*, *479*, 1320.

Bonev, T., Markov, H., Tomov, T., et al. 2017, *Bulg. Astron. J.*, *26*, 67.

Bosch-Ramon, V., Barkov, M. V., Mignone, A., & Bordas, P. 2017, *MNRAS*, *471*, L150.

Casares, J., Ribó, M., Ribas, I., Paredes, J. M., Vilardell, F., & Negueruela, I. 2012, *MNRAS*, *421*, 1103.

Casares, J., Negueruela, I., Ribó, M., Ribas, I., Paredes, J. M., Herrero, A., & Simón-Díaz, S. 2014, *Nature*, *505*, 378.

Chernyakova, M., & Malyshev, D. 2020, *Proc. Sci.*, *362*, 045.

Clarke, D. 1990, *A&A*, *227*, 151.

Corbet, R. H. D., Cheung, C. C., Kerr, M., et al. 2011, The Astronomer's Telegram, 3221.

Corbet, R. H. D., Chomiuk, L., Coe, M. J., et al. 2016, *ApJ*, *829*, 105.

Dubus, G. 2006, *A&A*, *456*, 801.

Dubus, G. 2013, *A&A*, *21*, 64.

Glebocki, R., Sikorski, J., Bielicz, E., & Krogulec, M. 1986, *Astron. Astrophys.*, *158*, 392.

Gutiérrez-Soto, J., Fabregat, J., Suso, J., Lanzara, M., Garrido, R., Hubert, A. M., & Floquet, M. 2007, *A&A*, *476*, 927.

Hanuschik, R. W. 1989, *Ap&SS*, *161*, 61.

Hanuschik, R. W. 1996, *A&A*, *308*, 170.

Hohle, M. M., Neuhäuser, R., & Schutz, B. F. 2010, *AN*, *331*, 349.

Johnston, S., Manchester, R. N., Lyne, A. G., Bailes, M., Kaspi, V. M., Qiao, G., & D'Amico, N. 1992, *ApJ*, *387*, L37.

Li, J., Torres, D. F., Cheng, K.-S., Wilhelmi, E. . O., Kretschmar, P., Hou, X., & Takata, J. 2017, *ApJ*, *846*, 169.

Lucarelli, F., Verrecchia, F., Striani, E., et al. 2010, The Astronomer's Telegram, 2761.

Lyne, A. G., Stappers, B. W., Keith, M. J., Ray, P. S., Kerr, M., Camilo, F., & Johnson, T. J. 2015, *MNRAS*, *451*, 581.

Martin, R. G., Tout, C. A., & Pringle, J. E. 2009, *MNRAS*, *397*, 1563.

Martin, R. G., Pringle, J. E., Tout, C. A., & Lubow, S. H. 2011, *MNRAS*, *416*, 2827.

Massi, M., & Jaron, F. 2013, *A&A*, *554*, A105.

Mathew, B., & Subramaniam, A. 2011, *Bull. Astron. Soc. India*, *39*, 517.

Mirabel, I. F. 2012, *Science*, *335*, 175.

Moritani, Y., Kawano, T., Chimasu, S., et al. 2018, *PASJ*, *70*, 61.

Negueruela, I. 2007, *ASP Conf. Ser.*, *367*, 477.

Paredes, J. M., & Bordas, P. 2019, *Rend. Lincei. Sci. Fis. Nat.*, *30*, 107.

Poeckert, R., & Marlborough, J. M. 1978, *ApJ*, *220*, 940.

Pols, O. R., Cote, J., Waters, L. B. F. M., et al. 1991, *A&A*, *241*, 419.

Reig, P. 2011, *Ap&SS*, *332*, 1.

Ribó, M., Munar-Adrover, P., Paredes, J. M., et al. 2017, *ApJ*, *835*, L33.

Ricker, G. R., Winn, J. N., Vanderspek, R., et al. 2015, *J. Astron. Telesc., Instrum. Syst.*, *1*, 014003.

Roberts, D. H., Lehar, J., & Dreher, J. W. 1987, *AJ*, *93*, 968.

Romero, G. E., Okazaki, A. T., Orellana, M., & Owocki, S. P. 2007, *A&A*, *474*, 15.

Smith, M. A., Henry, G. W., & Vishniac, E. 2006, *ApJ*, *647*, 1375.

Stellingwerf, R. F. 1978, *ApJ*, *224*, 953.

Straizys, V., & Kuriliene, G. 1981, *Ap&SS*, *80*, 353.

Tody, D. 1993, *ASP Conf. Ser.*, *52*, 173.

Wang, Y.-M., & Robertson, J. A. 1985, *A&A*, *151*, 361.

Williams, S. J., Gies, D. R., Matson, R. A., Touhami, Y., Grundstrom, E. D., Huang, W., & McSwain, M. V. 2010, *ApJ*, *723*, L93.

Yudin, R. V. 2001, *A&A*, *368*, 912.

Zamanov, R., Stoyanov, K., & Mart, J. 2016a, *Bulg. Astron. J.*, *24*, 40.

Zamanov, R. K., Stoyanov, K. A., Mart, J., et al. 2016b, *A&A*, *593*, A97.

Zamanov, R., Mart, J., & Garca-Hernández, M. T. 2017, *Bulg. Astron. J.*, *27*, 57.

AUTHOR BIOGRAPHY

R. K. Zamanov: MSc - Sofia University St. Kl. Ohridski (1989); PhD - National Astronomical Observatory Rozhen, Bulgaria (1997); fellow - Universidad de Jaen, Spain (2000); postdoc - Osservatorio Astronomico di Padova, Padova, Italy (2001–2003); postdoc research assistant - Astrophysics Research Institute, Liverpool John Moores University, UK (2003–2005); proffesor of astrophysics and stellar astronomy - Institute of Astronomy and NAO, Bulgarian Academy of Sciences (since 2012).

How to cite this article: Zamanov RK, Stoyanov KA, Mart J, Marchev VD, Nikolov YM. Radius, rotational period, and inclination of the Be stars in the Be/gamma-ray binaries MWC 148 and MWC 656. *Astron. Nachr*. 2021;342:531–537. https://doi.org/10.1002/asna.202123856